Lipin, a lipodystrophy and obesity gene

Jack Phan and Karen Reue*

Departments of Human Genetics and Medicine, David Geffen School of Medicine and Molecular Biology Institute, University of California, Los Angeles and VA Greater Los Angeles Healthcare System, Los Angeles, California 90073
*Correspondence: reuek@ucla.edu

Summary

Lipodystrophy and obesity represent extreme and opposite ends of the adiposity spectrum and have typically been attributed to alterations in the expression or function of distinct sets of genes. We previously demonstrated that lipin deficiency impairs adipocyte differentiation and causes lipodystrophy in the mouse. Using two different tissue-specific lipin transgenic mouse strains, we now demonstrate that enhanced lipin expression in either adipose tissue or skeletal muscle promotes obesity. This occurs through diverse mechanisms in the two tissues, with lipin levels in adipose tissue influencing the fat storage capacity of the adipocyte, and lipin levels in skeletal muscle acting as a determinant of whole-body energy expenditure and fat utilization. Thus, variations in lipin levels alone are sufficient to induce extreme states of adiposity and may represent a mechanism by which adipose tissue and skeletal muscle modulate fat mass and energy balance.

Introduction

Considerable inroads have been made in the last decade toward identifying and characterizing obesity genes expressed in adipose tissue and the hypothalamus. This has led to the formulation of the adipose-hypothalamic axis as a mechanism by which the CNS senses and regulates adipose tissue mass in the periphery (Flier, 2004; Havel, 2001; Schwartz et al., 2000; Seeley and Woods, 2003). The hypothalamus receives input from afferent adiposity signals, notably leptin, which communicate the status of body fat stores. These signals subsequently act to modulate energy balance to maintain a predetermined level of adiposity. In addition, substantial attention has focused on the neural circuitry upon which these peripheral signals act (Cummings and Schwartz, 2003; Seeley et al., 2004). This has led to the identification of a plethora of neurotransmitters and receptor systems with demonstrated and potential roles in regulating food intake and energy expenditure.

Efforts have also been applied to identify gene defects underlying conditions of insufficient adipose tissue, as is observed in lipodystrophy. As lipodystrophy and obesity represent extreme ends of the adiposity spectrum, it raises the question of whether genes whose deficiency leads to lipodystrophy may also promote obesity when overexpressed. Consistent with this possibility is the demonstration that some forms of congenital lipodystrophy in humans result from defects in genes with roles in adipogenesis (i.e., *PPARG*) and fat synthesis/storage (i.e., *AGPAT2*) (Garg, 2004). However, it is unknown whether genes such as these, which function directly in the adipose tissue, can also cause obesity. Here we demonstrate that lipin, which is expressed primarily in peripheral tissues, possesses this capacity, causing lipodystrophy in its absence and promoting obesity when its levels are enhanced.

Lipin, which is encoded by the *Lpin1* gene, was identified through positional cloning as the gene mutated in the fatty liver dystrophy (*fld*) mouse (Péterfy et al., 2001). Null mutation in lipin in these animals confers lipodystrophy, characterized by severe deficiency in adipose tissue mass, development of insulin resistance, and a progressive peripheral neuropathy (Langner et al., 1989; Reue et al., 2000). Lipin is expressed at high levels in metabolically active tissues such as adipose tissue and skeletal muscle and has been shown to interact with proteins having a putative role in nucleocytoplasmic transport in yeast, consistent with its nuclear localization in mammalian cells (Péterfy et al., 2001; Tange et al., 2002). We recently demonstrated that lipin deficiency prevents both diet-induced and genetic obesity and is required upstream of PPARγ for normal adipocyte differentiation (Phan et al., 2004). However, it is unclear by examining lipin deficiency whether elevated lipin levels could promote increased adiposity. In addition, the function of lipin in skeletal muscle, where it is expressed at levels comparable to those in adipose tissue, has not yet been explored. To better understand the effect of lipin levels in adipose tissue and skeletal muscle on fat mass and energy metabolism, we have generated and characterized transgenic mouse models with enhanced lipin expression in either mature adipocytes or skeletal muscle.

Results

Enhanced lipin expression in adipose tissue or skeletal muscle promotes obesity

To investigate the role of lipin specifically in mature adipocytes, we generated transgenic mice with enhanced lipin expression specifically in adipose tissue (aP2-lipin Tg) using the 5.4-kb enhancer/promoter region of the aP2 gene, which directs expression in terminally differentiated adipocytes (Graves et al., 1991; Ross et al., 1990). In addition, to investigate the effects of enhanced lipin expression in skeletal muscle, we produced a muscle-specific lipin transgenic mouse (Mck-lipin Tg) using the mouse muscle-creatine kinase promoter (Johnson et al., 1989; Manchester et al., 1996). Transgenic mice were generated on a pure C57BL/6J strain background to avoid genetic heterogeneity, and the aP2- and Mck-lipin transgenics were

therefore compared to a single combined group of non-transgenic C57BL/6J littermates derived from both colonies. The aP2-lipin Tg mice exhibited a significant 3.5-fold increase in lipin mRNA levels in white adipose tissue and a 20% increase in brown adipose tissue (not statistically significant), with no changes occurring in other tissues examined (skeletal muscle, heart, kidney, intestine; Supplemental Figure S1A available with this article online). In Mck-lipin Tg mice, lipin mRNA levels were increased significantly in skeletal muscle by 3-fold and by 20% in heart (not statistically significant) and were not altered in the other tissues examined (Supplemental Figure S1A).

On a chow diet, aP2-lipin Tg mice had body weights similar to non-Tg littermates, whereas Mck-lipin Tg mice exhibited elevated body weight by 10 weeks of age and developed mild obesity by 20 weeks of age (Figure 1A). When fed a high-fat diet for 6 weeks, both aP2-lipin Tg mice and Mck-lipin Tg mice showed accelerated weight gain, increasing their body weight by ~40%, compared to a ~20% increase in non-Tg mice (Figure 1B). The response to the high-fat diet was most pronounced in Mck-lipin Tg mice as these animals gained nearly 18 g and became markedly obese after 6 weeks on the diet (Figures 1B and 1C), compared to a 9.9 g increase in aP2-lipin Tg and 5.3 g increase in non-Tg mice. The accelerated weight gain was reflected by a near doubling of fat pad mass in subcutaneous, gonadal, and retroperitoneal depots in aP2-lipin Tg mice, and more than a doubling of the subcutaneous and near tripling of the gonadal and retroperitoneal fat pad mass in Mck-lipin Tg, compared to non-Tg mice. This was evident both when expressed as absolute fat pad mass (Figure 1D) and as a percent of body weight (Supplemental Figure S1B).

Similar to human subjects and other animal models with impaired adipose tissue function, lipin-deficient *fld* mice develop insulin resistance (Reue et al., 2000). The occurrence of obesity in Tg mice overexpressing lipin in either adipose tissue or muscle raised the question of whether these animals might also exhibit altered insulin sensitivity. On a chow diet, fasting glucose levels were similar between Mck-lipin Tg and non-Tg mice but were significantly reduced in aP2-lipin Tg mice despite their increased adiposity compared to non-Tg animals (Figure 1E). Feeding a high-fat diet increased glucose levels in both non-Tg and Mck-Tg mice compared to the chow diet, but Mck-Tg animals reached significantly higher levels than the non-Tg mice. Interestingly, aP2-lipin Tg mice maintained significantly lower glucose levels than non-Tg mice on the high fat diet. Fasting plasma insulin levels also revealed distinct effects of lipin overexpression in adipose tissue versus muscle. On a chow diet, Mck-lipin Tg mice had elevated insulin levels compared to the other two strains, which was severely exacerbated by the high-fat diet (Figure 1F). And although the high-fat diet elicited increased insulin levels over the chow values in both non-Tg and aP2-lipin Tg mice, the increase was significantly blunted in the aP2-lipin Tg animals, which reached levels of only 40% of those in non-Tg mice and less than 10% of the levels in Mck-lipin Tg mice. As an indicator of insulin resistance, we calculated the HOMA-IR (homeostatic model of assessment of insulin resistance), which largely mirrored the trends observed in insulin levels among the three strains. Thus, in parallel with the increased adipose tissue mass observed in Mck-lipin Tg mice, these animals exhibited significantly elevated HOMA-IR values on both chow and high-fat diets (Figure 1G). However, despite the increased fat mass in aP2-lipin Tg compared to non-Tg mice, these animals had reduced HOMA-IR values on the high-fat diet, indicating greater insulin sensitivity associated with increased lipin expression specifically in adipose tissue.

Enhanced lipin expression in adipose tissue, but not muscle, increases lipogenic gene expression

As we have previously determined that lipin deficiency severely impairs adipocyte differentiation and adipogenic gene expression (Phan et al., 2004), we investigated whether enhanced lipin expression promotes adipogenic gene expression. We examined adipose tissue gene expression in aP2-lipin Tg, Mck-lipin Tg, and non-Tg mice on the chow and high-fat diets. We found no effect of either the aP2-lipin or Mck-lipin transgenes on PPARγ or aP2 expression levels, indicating that obesity resulting from enhanced lipin expression in mature adipocytes or muscle is not associated with increased adipogenic gene expression (Figure 2A). Since the aP2-regulatory elements direct lipin expression in mature adipocytes but not preadipocytes, these results are consistent with a role for lipin in mature adipocytes that is distinct from its requirement in preadipocytes for induction of adipogenic gene expression.

Next, we examined the expression of lipid synthesis and storage genes in adipose tissue from Tg mice fed chow and high-fat diets. In chow-fed aP2-lipin Tg mice, we found a 3.9-fold increase compared to non-Tg mice in expression of DGAT (acyl CoA: diacylglycerol acyltransferase), a key enzyme in triglyceride synthesis (Figure 2B). After 6 weeks of the high-fat diet, adipose tissue from aP2-lipin Tg animals also exhibited elevated expression levels of acetyl-CoA carboxylase-1 (ACC-1), phosphoenolpyruvate carboxykinase (PEPCK), as well as DGAT, by a factor of 4.5, 2.6, and 3.9, respectively. Expression of fat synthesis/storage genes was not increased in adipose tissue from Mck-lipin Tg on either diet, indicating that enhanced expression of these genes in aP2-lipin Tg mice likely reflects elevated lipin levels in adipose tissue rather than increased adiposity per se.

Lipin levels in muscle are a determinant of energy expenditure and fuel selection

Previously, we showed that lipin-deficient mice exhibit normal food intake but reduced feed conversion efficiency (Phan et al., 2004). Similarly, food intake was not altered in aP2-lipin Tg or Mck-lipin Tg compared to non-Tg mice on either a chow (data not shown) or high-fat diet (Figure 3A). We did, however, observe an increase in feed conversion efficiency (weight gain per food intake normalized to food absorption; see Experimental procedures) in both transgenic strains (Figure 3B). These findings suggested that lipin levels may modulate energy expenditure.

To investigate this possibility, we examined oxygen consumption in *fld*, aP2-lipin Tg, and Mck-lipin Tg mice on chow and high-fat diets. Compared to wild-type mice, *fld* mice fed a chow diet exhibited significantly higher oxygen consumption in both light (~10% increase) and dark (~15% increase) phases (Figure 3C). The increase in oxygen consumption on the high-fat diet was approximately 20% and 15% during the light and dark phases, respectively (Supplemental Figure S2A). The opposite effect was seen in Mck-lipin Tg mice. Thus, on a chow diet, Mck-lipin Tg mice consumed about 10% less oxygen during both the light and dark cycles compared to non-Tg mice

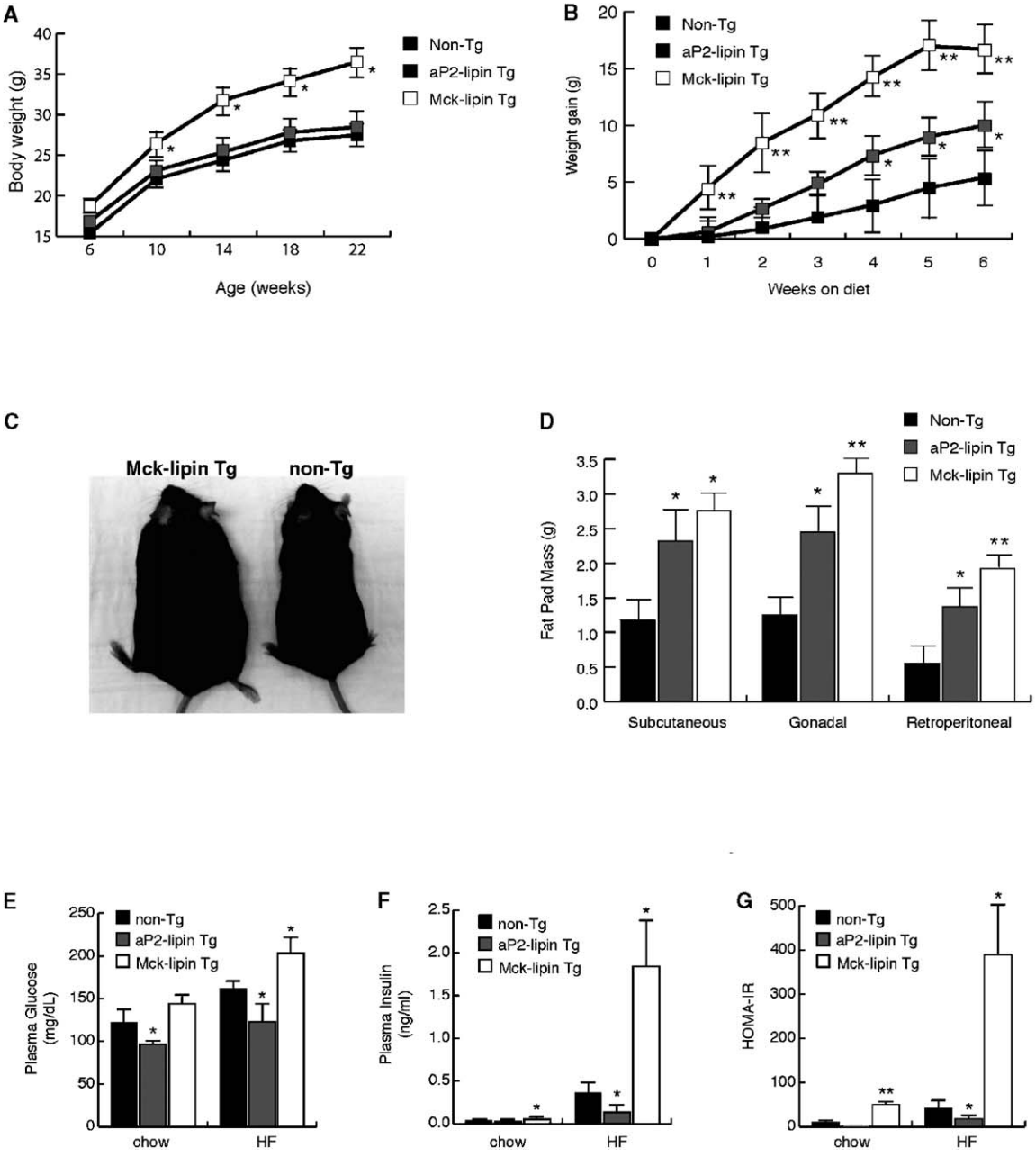

Figure 1. Increased adiposity and accelerated diet-induced obesity in lipin transgenic mice

A) Growth curves from 6 to 22 weeks of age for female mice (n = 6 for each genotype). Male mice showed a similar trend for higher body weight in Mck-lipin Tg mice from weeks 6–22, although statistical significance was not reached until the 24th week (not shown). *, $p < 0.01$ versus non-Tg and aP2-lipin Tg.

B) Weight gain in non-Tg, aP2-lipin-Tg, and Mck-lipin Tg mice fed a high-fat diet for 6 weeks. *, $p < 0.05$ and **, $p < 0.01$ versus non-Tg.

C) Female Mck-lipin Tg and non-Tg littermates at 6 months of age after 6 weeks on the high-fat diet.

D) Weights of subcutaneous, gonadal, and retroperitoneal fat pads, taken from 6-month-old male mice (n = 6 for each genotype) after 6 weeks on the high-fat diet. *, $p < 0.01$; **, $p < 0.001$ versus non-Tg. Similar differences in body weight and adiposity were obtained with female mice (not shown).

E) Fasting glucose levels in female mice (n = 6) at 6–8 months of age on a chow diet or after 6 weeks on a high-fat diet. *, $p < 0.05$ versus non-Tg.

F) Fasting insulin levels in mice described in (**E**). *, $p < 0.05$ versus non-Tg.

G) Insulin resistance expressed as HOMA-IR index calculated from values presented in (**E**) and (**F**) (see Experimental procedures). *, $p < 0.05$ and **, $p < 0.01$ versus non-Tg.

(Figure 3D). On the high-fat diet, energy expenditure in Mck-lipin Tg compared to non-Tg mice was reduced further by 15% in both light and dark phases (Supplemental Figure S2B). Despite enhanced adiposity in aP2-lipin Tg mice, there was no significant difference in energy expenditure, though there was a trend toward slightly reduced oxygen consumption on both chow and high-fat diets (Figure 3D and Supplemental Figure S2B). While the reduction in energy expenditure in the aP2-lipin

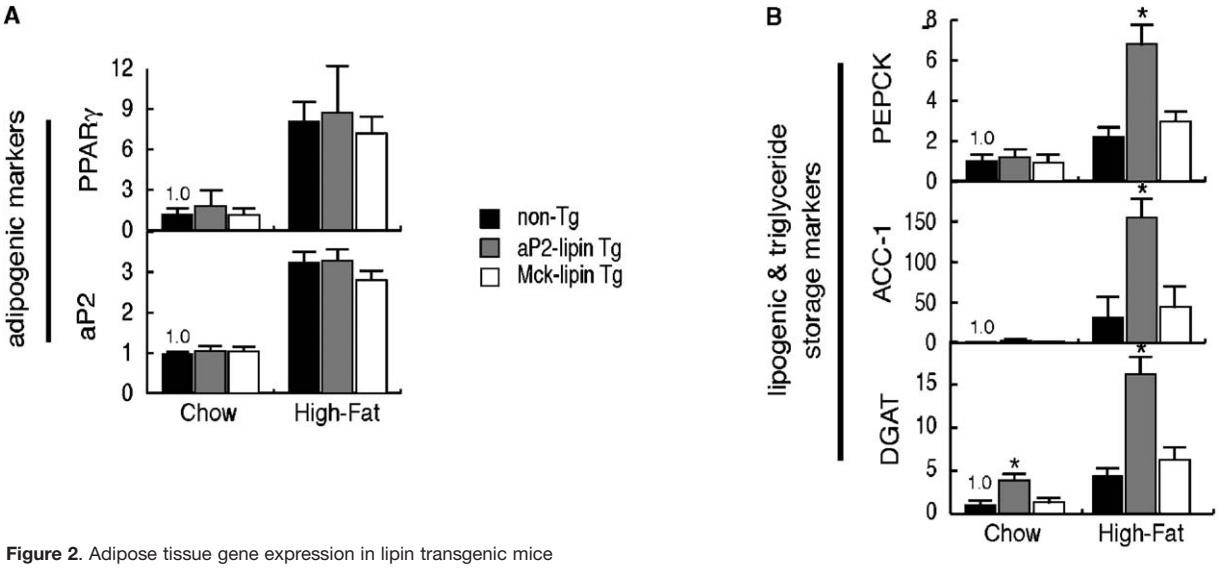

Figure 2. Adipose tissue gene expression in lipin transgenic mice

Expression of adipogenic (**A**) and lipogenic (**B**) genes determined by real-time RT-PCR analysis of reproductive fat pads taken from 4- to 5-month-old male mice fed a chow or high-fat diet (n = 6 for each genotype). Values for non-Tg mice were set to 1.0. *, $p < 0.01$ versus non-Tg and Mck-lipin Tg. DGAT, acyl CoA:diacylglycerol acyltransferase; ACC-1, acetyl Co-A carboxylase-1; PEPCK, phosphoenolpyruvate carboxykinase.

Tg mice was not statistically significant, it is possible that the modest reductions consistently observed nevertheless contribute to the positive energy balance in these animals.

Concordant with the increased energy expenditure in *fld* mice, body temperature was elevated in these animals (Figure 3E). This could not be accounted for by increased thermogenesis due to elevated uncoupling protein-1 (UCP-1) expression in brown adipose tissue, as *fld* mice express normal levels of UCP-1 mRNA (Figure 3F). In contrast to lipin-deficient mice, body temperature was decreased in Mck-lipin Tg mice but was not different from control values in aP2-lipin Tg mice. This was true on either a chow (Figure 3E) or high-fat diet (data not shown). As with the lipin-deficient mice, the altered body temperature in lipin Tg mice could not be explained by altered UCP-1 expression in brown adipose tissue on a chow (Figure 3F) or high-fat diet (data not shown). Thus, lipin levels in skeletal muscle but not adipose tissue appear to be a significant determinant of energy expenditure.

We also assessed the respiratory quotient (RQ) in lipin-deficient and lipin transgenic mice under ad libitum fed, fasting, and re-fed conditions to determine the effect of lipin levels on whole-body carbohydrate versus fat utilization. During ad libitum feeding conditions, RQ values were lower in *fld* compared to wild-type mice, indicating a preference for fat utilization in *fld* mice during conditions of continual food availability (Figure 4A). In contrast, ad libitum fed RQ values were higher in Mck-lipin Tg, but not aP2-lipin Tg, when compared to non-Tg mice (Figure 4B).

Upon fasting, RQ values in humans and mice normally decrease to indicate a shift away from glucose and toward fatty acid utilization. Although RQ values declined in *fld* mice after an overnight fast, they remained higher than wild-type mice (Figure 4A). This likely reflects the decreased availability of fatty acid substrates in lipin-deficient mice due to impaired adipose tissue development. This is supported by the observation that re-feeding for 6 hr re-established the preference for fat utilization in *fld* compared to wild-type mice observed during ad libitum feeding conditions (Figure 4A). In contrast to lipin-deficient mice, the Mck-lipin Tg mice exhibited elevated RQ under all conditions, indicating a failure to utilize fat as efficiently as non-Tg or aP2-lipin Tg mice (Figure 4B). Even upon fasting, Mck-lipin Tg mice maintained higher RQ values than non-Tg and aP2-lipin Tg mice, which were similar to each other. The abundance of fat stores in Mck-lipin Tg mice suggests that higher fasting RQ in these mice may reflect resistance to fasting-induced lipolysis and β-oxidation rather than decreased substrate availability (Bezaire et al., 2001; Kelley et al., 1999; Owen et al., 1979). The abnormal RQ values observed in *fld* and MCK-lipin Tg mice cannot be attributed to differences in long-term or acute food consumption, as food intake was similar to that of wild-type and nontransgenic animals (Figures 3A and 4C and Phan et al., [2004]). Thus, whereas lipin deficiency leads to an increase in the proportional utilization of fatty acid compared to glucose substrates for oxidation, enhanced lipin levels in skeletal muscle produced the opposite effect of decreased fatty acid utilization.

Lipin deficiency and enhanced expression in muscle have opposite effects on fatty acid metabolism gene expression

To examine the molecular basis for altered fuel partitioning in lipin-deficient and lipin transgenic mice, we measured the expression of several fatty acid metabolism genes in skeletal muscle. In *fld* compared to wild-type mice, we observed nearly double the levels of fatty acid oxidation gene expression, including carnitine palmitoyl transferase-1 (CPT-1) and acyl-CoA-oxidase (AOX), and a 50% reduction in acetyl-CoA-carboxylase (ACC), responsible for production of malonyl CoA, which inhibits fatty acid oxidation (Figure 5A). On the other hand, expression levels for genes associated with lipid storage, such as DGAT and ATP-citrate lyase (ACL), were decreased in *fld* muscle. Examination of Mck-lipin Tg mice revealed an op-

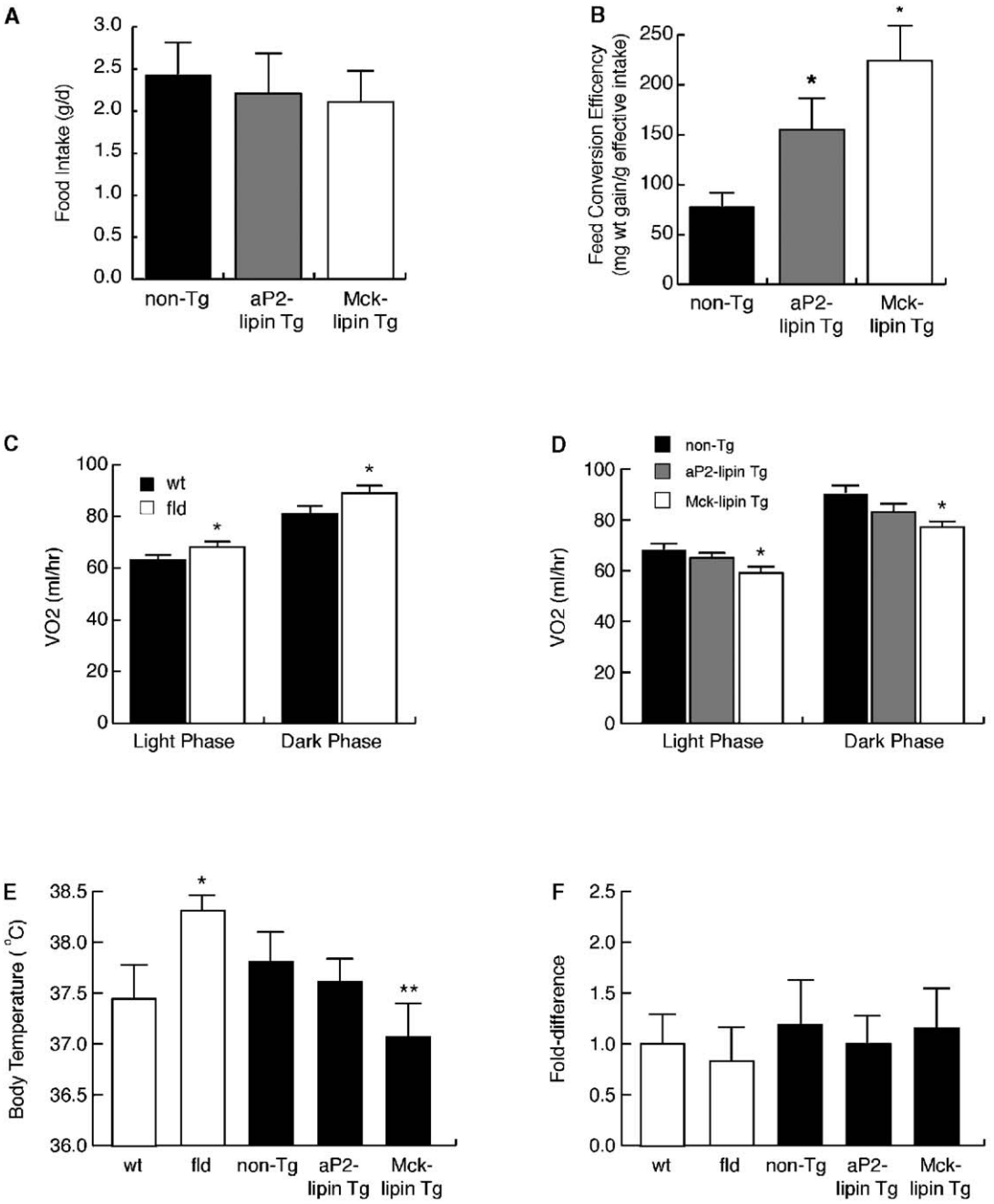

Figure 3. Lipin levels are a determinant of whole-body energy expenditure

A) Daily food intake in animals from Figure 1B.

B) Feed conversion efficiency for animals in Figure 1B, calculated from the weight gain per effective food intake after 6 weeks on the high-fat diet. *, $p < 0.01$ versus non-Tg.

C) Average oxygen consumption (VO_2, expressed as ml/hr) was determined via indirect calorimetry during the light (12pm–6pm) and dark (6pm–12am) period for 6-month-old female wild-type and *fld* mice on a chow diet (n = 6 for each genotype). *, $p < 0.01$ versus wild-type.

D) Average VO_2 during the light and dark phase for 5- to 7-month-old female non-Tg, aP2-lipin Tg, and Mck-lipin Tg mice on a chow diet (n = 5 for each genotype). *, $p < 0.01$ versus non-Tg and aP2-lipin Tg.

E) Rectal body temperature measured in 5- to 7-month-old female mice (n = 8 for each genotype). *, $p < 0.05$ versus wild-type (wt); **, $p < 0.05$ versus non-Tg. Similar differences in VO_2 and body temperature were obtained with male mice (not shown). Note that differences between wild-type and non-Tg oxygen consumption and body temperature values, although not significant, may be due to differences in the background strain (BALB/cByJ versus C57BL/6J, respectively).

F) UCP-1 mRNA levels in brown adipose tissue from female mice (n = 5) at 6 months of age determined by real-time RT-PCR. Values for wild-type mice were set to 1.0.

posite pattern of expression compared to *fld* mice, with nearly a 50% reduction in expression of fatty acid oxidation genes (CPT-1 and AOX), and double to triple the non-Tg levels of ACC, DGAT, and ACL (Figure 5B). We did not observe any differences in fatty acid metabolism gene expression in skeletal muscle of aP2-lipin Tg compared to non-Tg mice (Figure 5B). Thus, associated with the observed differences in RQ measurements are changes in muscle gene expression that favor

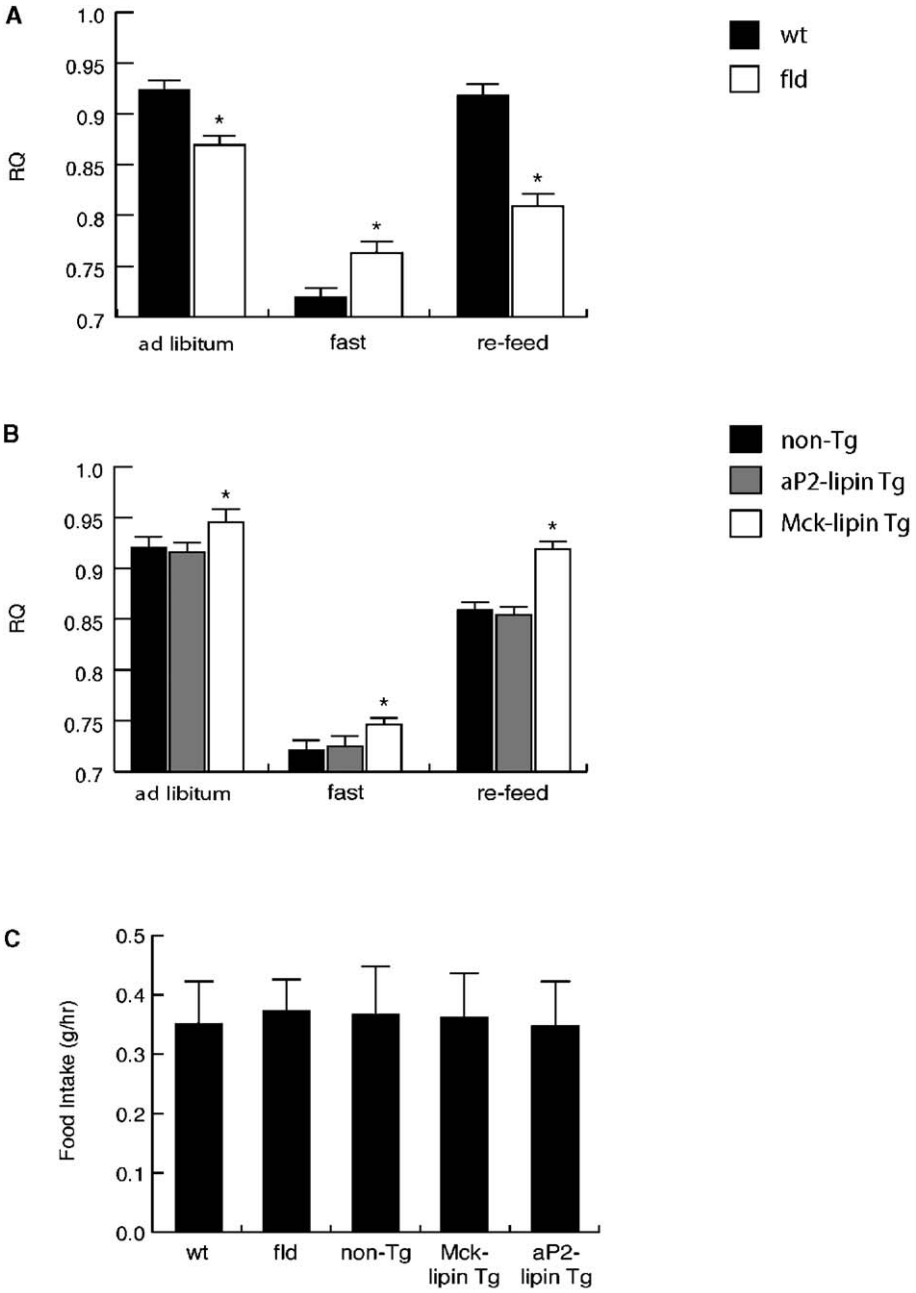

Figure 4. Lipin levels influence metabolic fuel selection

Respiratory quotient (RQ) values were determined from 6-month-old female mice (n = 6 for each genotype) under the following feeding conditions: fed ad libitum, fasted 12 hr, or re-fed for 6 hr after 12-hr fast.

A) Increased relative fat oxidation in lipin-deficient mice during fed states. *, $p < 0.01$ versus wild-type.

B) Attenuation of relative fat oxidation in Mck-lipin Tg but not aP2-lipin Tg mice. *, $p < 0.01$ versus non-Tg or aP2-lipin Tg.

C) Acute food consumption measured for 4 hr after a 12-hr fast in animals from (**A**) and (**B**).

fatty acid utilization over storage in *fld* mice, with an opposite expression profile that favors fatty acid storage in Mck-lipin Tg mice.

Lipin replacement in muscle of lipin-deficient mice normalizes energy expenditure and fuel utilization but not adipose tissue accumulation

Data from our *fld* and Mck-lipin Tg mice strongly implicate lipin levels in skeletal muscle as a determinant of energy expenditure and fatty acid utilization. To ascertain whether the altered energy metabolism observed in *fld* mice is attributable specifically to the lack of lipin in muscle (as opposed to adipose or other tissues where lipin is expressed), we restored lipin expression in skeletal muscle of *fld* mice by introducing the Mck-lipin transgene. The resulting *fld*-Mck-lipin Tg mice exhibit lipin deficiency in all tissues except skeletal muscle, where lipin levels are increased by a factor of 2.6 above wild-type levels, similar to those in Mck-lipin Tg animals (data not shown). Examination of energy expenditure in *fld*-Mck-lipin Tg mice revealed decreased oxygen consumption compared to *fld* mice, with values only slightly higher than those observed in Mck-lipin Tg mice (Figure 6A). In addition, body temperature was reduced and RQ values were elevated to levels observed in Mck-lipin Tg mice by restoration of lipin expression exclusively in muscle of *fld* mice (Figures 6B and 6C). This was accompanied by corresponding changes in gene expression in skeletal

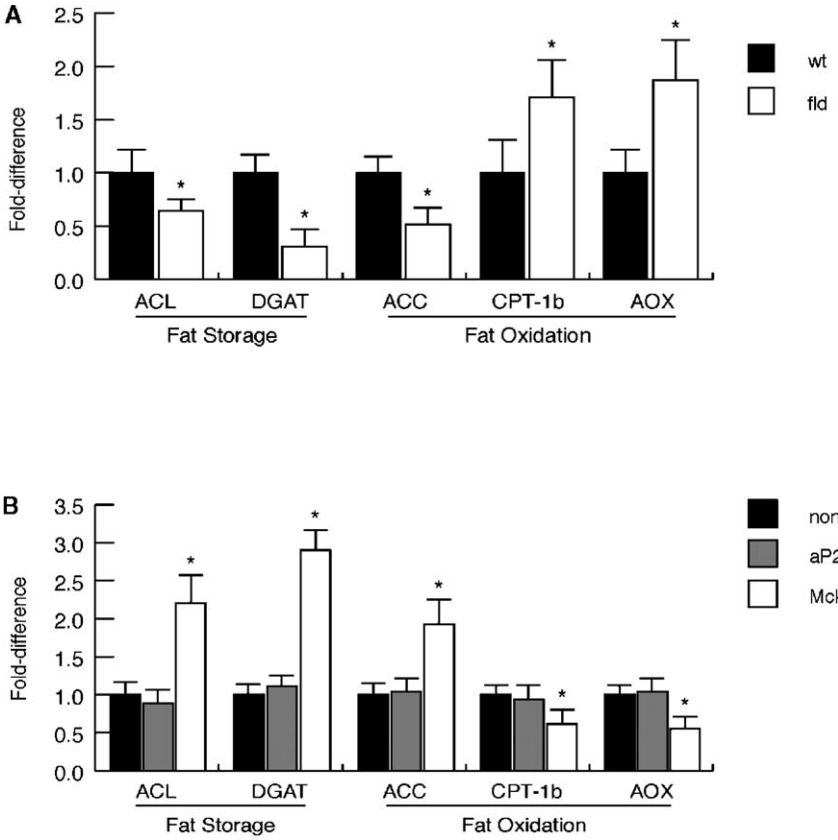

Figure 5. Gene expression profile in muscle of lipin-deficient and lipin transgenic mice reflects altered energy metabolism

A) Real-time RT-PCR analysis of gene expression in skeletal muscle taken from 12-hr fasted, 7-month-old *fld* and wild-type (wt) mice after 6 weeks on the high-fat diet (n = 5 for each genotype). *, $p < 0.01$ versus wild-type.

B) Real-time RT-PCR analysis of gene expression in skeletal muscle taken from 12-hr fasted, 6-month-old female non-Tg, aP2-lipin Tg, and Mck-lipin Tg mice after 6 weeks on high-fat diet (n = 6 for each genotype). *, $p < 0.01$ versus non-Tg and aP2-lipin Tg. ACL, ATP-citrate lyase; DGAT, acyl CoA:diacylglycerol acyltransferase; ACC-1, acetyl Co-A carboxylyase-1; CPT-1b, carnitine palmitoyl transferase-1b; AOX, acyl-CoA-oxidase.

muscle from *fld*-Mck-lipin Tg mice, showing decreased expression of CPT-1 and AOX and increased expression of ACC, ACL, and DGAT (Figure 6D). Interestingly, despite decreased energy expenditure and suppression of fatty acid utilization in *fld*-Mck-lipin Tg mice, these mice exhibited no increase in body weight or adiposity compared to *fld* mice and were resistant to diet-induced obesity (Figures 6E and 6F). This is attributable in part to the absence of lipin in the adipose tissue of *fld*-Mck-lipin Tg mice, impairing the capacity to develop normal adipocytes and thus store fat. Consistent with this interpretation, PPARγ, aP2, and DGAT mRNA levels were dramatically reduced in adipose tissue from *fld*-Mck-lipin Tg (Figure 6G). Overall, these results establish lipin levels in skeletal muscle as a major determinant of whole-body energy expenditure and fatty acid utilization and confirm the requirement for lipin in adipose tissue in order to develop normal fat mass.

Discussion

Our studies in lipin-deficient and lipin transgenic mice reveal that modulation of lipin levels alone is sufficient to cause dramatic shifts in adiposity, resulting in either lipodystrophy in the absence of lipin or obesity due to enhanced lipin expression in either adipose tissue or skeletal muscle. Moreover, these studies reveal that lipin levels in two metabolically important tissues, adipose tissue and skeletal muscle, modulate fat mass by distinct mechanisms. The effects of altered lipin levels on adiposity are opposite to those conferred by altered leptin levels, where leptin deficiency causes obesity and elevated leptin levels produced by overexpression in liver cause a lean phenotype (Friedman, 2002; Ogawa et al., 1999). However, although both lipin and leptin are synthesized in peripheral tissues, a major distinction is that leptin exerts its primary effects through signaling in the hypothalamus, while lipin is not secreted and therefore exerts its effects on adiposity and energy balance through an as yet unknown intracellular function in adipose tissue and skeletal muscle.

In adipose tissue, we previously demonstrated that lipin expression in the adipocyte occurs in two phases—a transient induction in preadipocytes shortly after stimulation with adipogenic factors and a second wave of expression in mature adipocytes that have accumulated triglyceride (Phan et al., 2004). The requirement for lipin in pre-adipocytes for normal adipocyte differentiation contributes to the lack of normal fat accumulation in *fld* and *fld*-Mck-lipin Tg mice, but the role of lipin in mature adipocytes could not be addressed in lipin-deficient animals as their adipose tissue remains immature. Using the aP2-lipin transgene to drive lipin expression in mature adipocytes, we show that enhanced lipin expression in mature adipocytes augments adiposity and accelerates diet-induced obesity. This is in part due to enhanced feed efficiency and increased triglyceride synthesis. The aP2-lipin transgene did not, however, affect adipogenic gene expression, consistent with the proposal that the two temporal phases of lipin gene expression have distinct roles in adipocyte biology.

Skeletal muscle, by virtue of its mass, is a major determinant

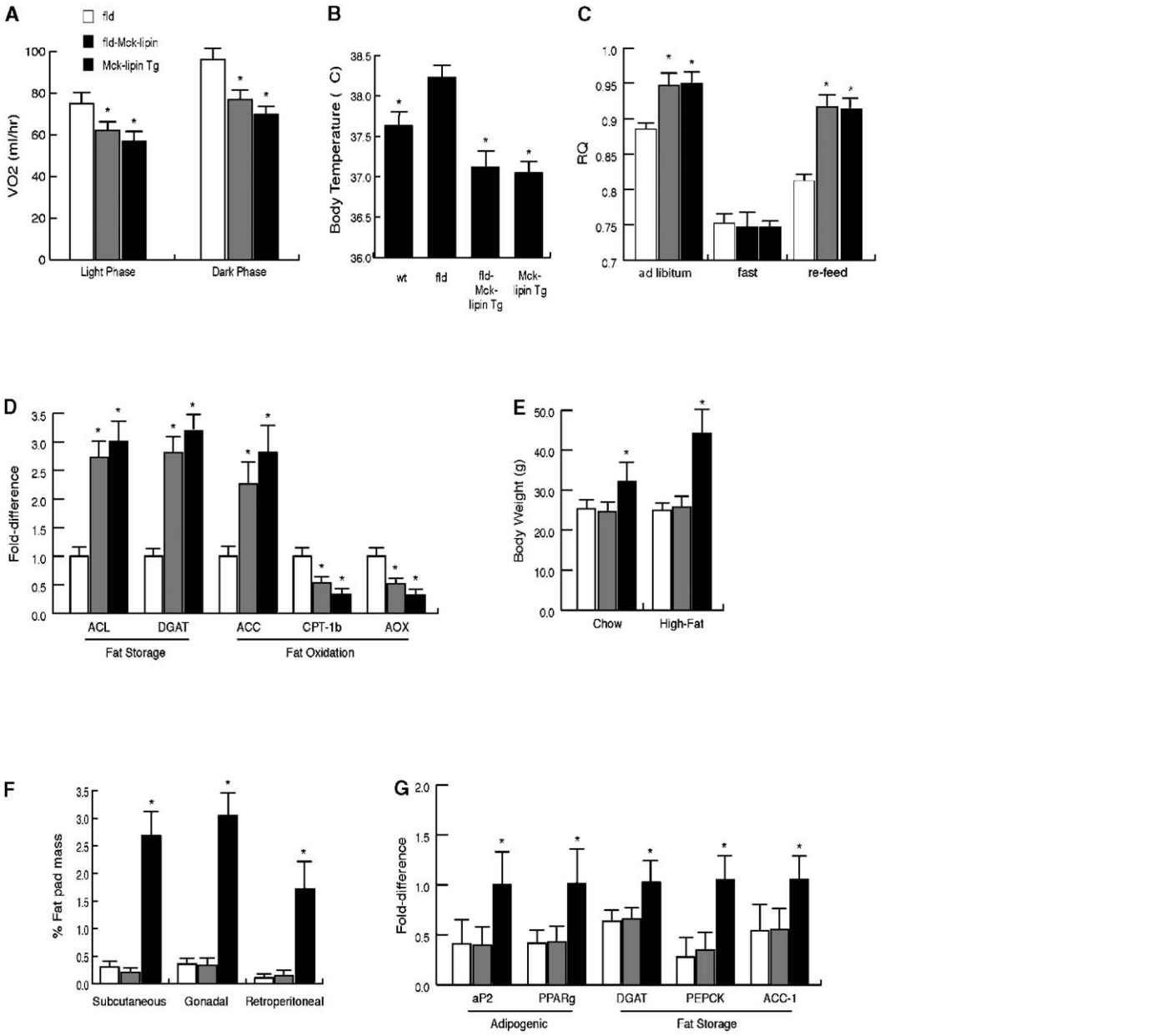

Figure 6. Effect of lipin deficiency on energy metabolism is reversed by restoration of lipin expression in skeletal muscle

A–C) Oxygen consumption, body temperature, and RQ were measured in chow-fed *fld*, *fld*-MCK-lipin, and Mck-lipin Tg mice as in Figure 3. Measurements were performed in 4- to 6-month-old male mice (n = 6 for each genotype). *, $p < 0.01$ versus *fld*.

D) Muscle gene expression was determined by real-time RT-PCR. *, $p < 0.01$ versus *fld*.

E) Body weight of male mice aged 4–6 months on a chow or after 6 weeks on a high-fat diet (n = 4 for each genotype). *, $p < 0.05$ versus *fld* and *fld*-Mck-lipin Tg.

F) Fat pad mass normalized to body weight of male mice aged 5–7 months after 6 weeks on a high-fat diet (n = 4 for each genotype). *, $p < 0.001$ versus *fld* and *fld*-Mck-lipin Tg.

G) Adipose tissue gene expression determined by real-time RT-PCR. Gene abbreviations are the same as in Figures 2 and 5. *, $p < 0.05$ versus *fld* and *fld*-Mck-lipin Tg.

of whole-body fatty acid utilization. However, the identification of genes that regulate energy expenditure and thermogenesis in this organ has been elusive. The discovery of UCP-3 provided an attractive candidate for a modulator of energy expenditure in skeletal muscle. UCP-3 is highly expressed in skeletal muscle and when overexpressed, produces lean and hyperphagic mice (Clapham et al., 2000; Son et al., 2004). However, the lack of an observable phenotype in mice deficient for UCP-3 indicated an alternative function for UCP-3 in this tissue (Gong et al., 2000; Vidal-Puig et al., 2000). In contrast, lipin appears to satisfy these criteria as a modulator of whole-body energy expenditure and fatty acid partitioning in muscle, with lipin deficiency and enhanced lipin expression in muscle producing opposite effects on energy expenditure and fatty acid utilization.

Enhanced lipin expression in adipose tissue and skeletal muscle had distinct effects on glucose homeostasis and insulin sensitivity. Thus, whereas lipin overexpression in muscle produced obesity-associated insulin resistance, enhanced lipin expression in mature adipocytes improved insulin sensitivity over that in non-Tg mice despite increased adiposity. It has

been suggested that preferential fatty acid uptake and triglyceride storage specifically in adipose tissue may prevent lipid deposition ectopically in tissues such as muscle or pancreatic β cells, thus improving whole-body insulin sensitivity (Frayn, 2002). Such a mechanism might explain the improved insulin sensitivity in the face of moderate obesity that is observed in transgenic mice overexpressing DGAT in adipose tissue (Chen et al., 2002). Given the increased DGAT expression in adipose tissue of aP2-lipin Tg animals, increased fatty acid trapping may contribute to the enhanced insulin sensitivity in these animals as well, though additional effects on adipose tissue function may also have a role.

Our results indicate that variations in lipin levels have dramatic effects on the expression of genes involved in adipogenesis as well as fatty acid synthesis, storage, and/or oxidation. Our preliminary studies indicate that lipin does not appear to act as a transcription factor, but evidence from the fission yeast lipin homolog suggests potential involvement in nucleocytoplasmic transport and/or nuclear envelope function (Tange et al., 2002). Consistent with this possibility, nuclear envelope structure and function have been shown to play an important role in determining the transcriptional state of groups of genes (Casolari et al., 2004). This raises the possibility that lipin may have a novel molecular role in regulating gene expression. On the other hand, the manner by which lipin levels in skeletal muscle determine fuel partitioning may extend beyond its influence on gene expression. Since patterns of fatty acid utilization are related to muscle fiber type, with slow twitch (type I) muscle fibers having a higher capacity for fatty acid oxidation than fast twitch (type 2b) glycolytic muscle fibers (Dyck et al., 1997), it is possible that lipin levels in muscle may alter fuel utilization by influencing fiber type determination, as has been observed in mice with enhanced expression of PPARγ coactivator 1α (Lin et al., 2002). Precedent for a developmental role by lipin is seen in its requirement for normal adipocyte differentiation (Phan et al., 2004).

In summary, our studies demonstrate that modulation of lipin expression levels *(i.e.*, null, normal, and elevated specifically in adipose tissue or skeletal muscle) leads to dramatic alterations in adiposity, ranging from 10% to triple the normal amount of adipose tissue mass. Based on these results, the human *LPIN1* gene may be a candidate gene for disorders associated with not only decreased but also increased adipose tissue mass. In the extreme case, *LPIN1* null mutations could result in a lipodystrophy syndrome such as is seen in *fld* mice. In addition, more subtle genetic variations in lipin expression levels may contribute to the range of adiposity in human populations. Finally, unlike many obesity-related genes, lipin is predominantly expressed in and exerts its actions on peripheral tissues and, thus, may be a novel peripheral target for the treatment of obesity and/or lipodystrophy.

Experimental procedures

Mice and diets

Mice, ages 4–7 months for *fld,* aP2-Lipin Tg, and Mck-lipin Tg studies, were fed a standard laboratory chow diet (Purina 5001) or high-fat–high-carbohydrate diet containing 35% fat and 33% carbohydrate (Diet F3282, Bio-Serve, Frenchtown, New Jersey). To generate aP2-lipin and Mck-lipin transgenic mice, lipin cDNA (transcript variant 2, GenBank accession NM_015763) was cloned downstream of either the 5.4-kb aP2 promoter/enhancer (Graves et al., 1991; Ross et al., 1990) or the muscle creatine kinase (Mck) promoter (Johnson et al., 1989; Manchester et al., 1996), respectively, and upstream of an SV40 intron/poly (A) sequence (Liu et al., 2003). The transgene construct was microinjected into fertilized mouse C57BL/6J oocytes. Lipin transgenic animals were screened by PCR using primers that specifically detect the transgene but not endogenous lipin (aP2-Lipin Tg [gatacagggtctggtcatgaagg; ctgatcgttgtcagtctct]; Mck-Lipin Tg [ctggactacatagggtttcaggc, ctgatcgttgtcagtctct]). The transgenic founder lines were maintained by mating hemizygous animals to C57BL/6J partners. Since all mice were on a pure C57BL/6J background, control animals consisted of non-Tg C57BL/6J littermates derived from the two transgenic colonies combined into a single group. No differences were ever noted between non-Tg littermates derived from aP2-lipin Tg or Mck-lipin Tg colonies. Note that animal studies were performed on *fld* and wild-type mice from a BALB/cByJ background, and aP2-lipin Tg, Mck-lipin Tg, and non-Tg mice from a C57BL/6J background. Thus, slight variations between wild-type and non-Tg values may reflect strain-specific differences.

Glucose and insulin determinations

Blood was collected from mice after a 12 hr overnight fast under isoflurane anesthesia. Glucose levels were determined using a One Touch Ultra Blood Glucose Monitor (Lifescan). Insulin levels were determined with an ultrasensitive murine enzyme immunoassay (ALPCO Diagnostics, Windham, Massaschusetts). HOMA-IR, an index of insulin resistance, was calculated as the product of fasting glucose (mmol/l) and insulin (μU/ml) divided by 22.5 (Matthews et al., 1985).

Feed conversion efficiency and adipose tissue measurements

Food intake was determined over 10 days of ad libitum feeding in 5-month-old mice. Acute food intake after a 12 hr fast was measured every hr over a period of 6 hr. Feed conversion efficiency was calculated as the weight gain per effective food intake (food consumption normalized for fecal lipid output). Fecal lipid content was determined by quantitation of triglycerides and fatty acids in lipid extracts prepared from dried feces (Carr et al., 1993). Fat pads (inguinal subcutaneous, gonadal, and retroperitoneal) were dissected and weighed after conclusion of the high-fat diet or at 5 months of age in chow-fed mice.

RNA quantitation

Total RNA was isolated from adipose tissue or muscle with Trizol (Invitrogen), and treated with RNase-free DNase (Ambion) to remove any contaminating genomic DNA. First-strand cDNA synthesis was performed using oligo dT primers (Invitrogen). Real-time PCR reactions were performed on the iCycler iQ real-time detection system (BioRad) using SYBR Green PCR QuantiTect reagent kit (Qiagen). Each assay included (in triplicate) a standard curve of four serial dilution points of control cDNA (ranging from 100 ng to 100 pg), a no template control, and 25–50 ng of each sample cDNA. The relative concentrations of the endogenous controls TBP (TATA box binding protein) and HPRT (hypoxanthine phosphoribosyltransferase) and genes of interest were determined by plotting the threshold cycle (C_t) versus the log of the serial dilution points, and relative expression of gene of interest was determined after normalizing to endogenous controls. Primers used for real-time PCR were as follows: PPARγ (ccagagcatggtgccttcgct; cagcaaccattgggtcagctc); aP2 (gaacctggaagcttgtcttcg; accagcttgtcaccatctcg); DGAT (tgctacgacgagttcttgag; ctctgccacagcattgagac); ACC-1 (gcctcttcctgacaaacgag, tgactgccgaaacatctctg); PEPCK (cagctgctgcagaacacaagg, gctaactgctacagctaacgtg); ACL (ctcacacggaagctcatcaa, acgccctcatagacaccatc); CPT-1b (gtcgcttcttcaaggtctgg, aagaaagcagcacgttcgat); AOX (caggaagagcaaggaagtgg, ccttttctggctgatcccata); TBP (acccttcaccaatgactcctatg; atgatgactgcagcaaatcgc); HPRT (cacaggactagaacacctgc; gctggtgaaaaggacctct); UCP-1 (gggcccttgtaaacaacaaa; gtcggtccttccttggtgta).

Indirect calorimetry and core body temperature

Oxygen consumption (VO_2) and carbon dioxide production were measured using a one-chamber Oxymax indirect calorimetry system (Columbus Instruments, Columbus, Ohio). Temperature was maintained at 22°C –24°C, and lights were on from 6:00 to 18:00. Food was removed during the light cycle (6:00–18:00) and replaced and available ad libitum throughout the dark phase. Oxymax system settings were as follows: air flow rate of 0.6 l/min, sample flow rate of 0.5 l/min, settling time of 6 min, and measuring time of 3 min. VO_2 is expressed as milliliter per hour. Data normalized to body

weight or to body weight (in kg) raised to the 0.75 power all showed the same relationships and significant differences as those not normalized to body weight (data not shown). Data from the initial 3 hr were excluded from calculations to allow animals time to settle. VO_2 measurements were taken every 3 min and averaged over each subsequent 60 min period.

The respiratory quotient (RQ) is the ratio of liters carbon dioxide produced to liters oxygen consumed. The oxidation of carbohydrate exclusively results in an RQ of 1.00, whereas the oxidation of fatty acids results in a value of $\sim$0.70 . For each mouse, RQ values were recorded at the same time points used for oxygen consumption determinations. For ad libitum conditions, mice had free access to food during the entire measurement. For fasted mice, food was taken away at 6:00 and replaced at 18:00 to begin the re-feeding period.

Core body temperature was measured in all animals using a Ret-3 mouse rectal probe attached to a BAT-10 multipurpose digital thermometer (Physitemp Instruments Inc., Clifton, New Jersey).

Statistical analysis

The number of mice in each experimental group is indicated in the figure legends. A two-tailed Student's t test was used to calculate p values. All values are presented as mean ± SEM.

Supplemental data

Supplemental data includes two figures and can be found with this article online at http://www.cellmetabolism.org/cgi/content/full/1/1/73/DC1/.

Acknowledgments

We wish to thank Ping Xu for indispensable technical assistance and Miklós Péterfy for helpful discussions. This work was supported by National Institutes of Health grant HL28481 and the UCLA Medical Scientist Training Program grant GM08042.

Received: October 5, 2004
Revised: December 17, 2004
Accepted: December 17, 2004
Published: January 19, 2005

References

Bezaire, V., Hofmann, W., Kramer, J.K., Kozak, L.P., and Harper, M.E. (2001). Effects of fasting on muscle mitochondrial energetics and fatty acid metabolism in Ucp3(–/–) and wild-type mice. Am. J. Physiol. Endocrinol. Metab. *281*, E975–E982.

Carr, T.P., Andresen, C.J., and Rudel, L.L. (1993). Enzymatic determination of triglyceride, free cholesterol, and total cholesterol in tissue lipid extracts. Clin. Biochem. *26*, 39–42.

Casolari, J.M., Brown, C.R., Komili, S., West, J., Hieronymus, H., and Silver, P.A. (2004). Genome-wide localization of the nuclear transport machinery couples transcriptional status and nuclear organization. Cell *117*, 427–439.

Chen, H., Stone, S., Zhou, P., Buhman, K., and Farese, R.V., Jr. (2002). Dissociation of obesity and impaired glucose disposal in mice overexpressing acyl coenzyme A:diacylglycerol acyltransferase 1 in white adipose tissue. Diabetes *51*, 3189–3195.

Clapham, J.C., Arch, J.R., Chapman, H., Haynes, A., Lister, C., Moore, G.B., Piercy, V., Carter, S.A., Lehner, I., Smith, S.A., et al. (2000). Mice overexpressing human uncoupling protein-3 in skeletal muscle are hyperphagic and lean. Nature *406*, 415–418.

Cummings, D.E., and Schwartz, M.W. (2003). Genetics and pathophysiology of human obesity. Annu. Rev. Med. *54*, 453–471.

Dyck, D.J., Peters, S.J., Glatz, J., Gorski, J., Keizer, H., Kiens, B., Liu, S., Richter, E.A., Spriet, L.L., van der Vusse, G.J., and Bonen, A. (1997). Functional differences in lipid metabolism in resting skeletal muscle of various fiber types. Am. J. Physiol. *272*, E340–E351.

Flier, J.S. (2004). Obesity wars: molecular progress confronts an expanding epidemic. Cell *116*, 337–350.

Frayn, K. (2002). Adipose tissue as a buffer for daily lipid flux. Diabetologia *45*, 1201–1210.

Friedman, J.M. (2002). The function of leptin in nutrition, weight, and physiology. Nutr. Rev. *60*, S1–S14.] discussion S68–S84, S85–S87.

Garg, A. (2004). Acquired and inherited lipodystrophies. N. Engl. J. Med. *350*, 1220–1234.

Gong, D.W., Monemdjou, S., Gavrilova, O., Leon, L.R., Marcus-Samuels, B., Chou, C.J., Everett, C., Kozak, L.P., Li, C., Deng, C., et al. (2000). Lack of obesity and normal response to fasting and thyroid hormone in mice lacking uncoupling protein-3. J. Biol. Chem. *275*, 16251–16257.

Graves, R.A., Tontonoz, P., Ross, S.R., and Spiegelman, B.M. (1991). Identification of a potent adipocyte-specific enhancer: involvement of an NF-1-like factor. Genes Dev. *5*, 428–437.

Havel, P.J. (2001). Peripheral signals conveying metabolic information to the brain: short-term and long-term regulation of food intake and energy homeostasis. Exp. Biol. Med. (Maywood) *226*, 963–977.

Johnson, J.E., Wold, B.J., and Hauschka, S.D. (1989). Muscle creatine kinase sequence elements regulating skeletal and cardiac muscle expression in transgenic mice. Mol. Cell. Biol. *9*, 3393–3399.

Kelley, D.E., Goodpaster, B., Wing, R.R., and Simoneau, J.A. (1999). Skeletal muscle fatty acid metabolism in association with insulin resistance, obesity, and weight loss. Am. J. Physiol. *277*, E1130–E1141.

Langner, C.A., Birkenmeier, E.H., Ben-Zeev, O., Schotz, M.C., Sweet, H.O., Davisson, M.T., and Gordon, J.I. (1989). The fatty liver dystrophy (*fld*) mutation. A new mutant mouse with a developmental abnormality in triglyceride metabolism and associated tissue-specific defects in lipoprotein lipase and hepatic lipase activities. J. Biol. Chem. *264*, 7994–8003.

Lin, J., Wu, H., Tarr, P.T., Zhang, C.Y., Wu, Z., Boss, O., Michael, L.F., Puigserver, P., Isotani, E., Olson, E.N., et al. (2002). Transcriptional co-activator PGC-1 alpha drives the formation of slow-twitch muscle fibres. Nature *418*, 797–801.

Liu, X., Rossmeisl, M., McClaine, J., Riachi, M., Harper, M.E., and Kozak, L.P. (2003). Paradoxical resistance to diet-induced obesity in UCP1-deficient mice. J. Clin. Invest. *111*, 399–407.

Manchester, J., Skurat, A.V., Roach, P., Hauschka, S.D., and Lawrence, J.C., Jr. (1996). Increased glycogen accumulation in transgenic mice overexpressing glycogen synthase in skeletal muscle. Proc. Natl. Acad. Sci. USA *93*, 10707–10711.

Matthews, D.R., Hosker, J.P., Rudenski, A.S., Naylor, B.A., Treacher, D.F., and Turner, R.C. (1985). Homeostasis model assessment: insulin resistance and beta-cell function from fasting plasma glucose and insulin concentrations in man. Diabetologia *28*, 412–419.

Ogawa, Y., Masuzaki, H., Hosoda, K., Aizawa-Abe, M., Suga, J., Suda, M., Ebihara, K., Iwai, H., Matsuoka, N., Satoh, N., et al. (1999). Increased glucose metabolism and insulin sensitivity in transgenic skinny mice overexpressing leptin. Diabetes *48*, 1822–1829.

Owen, O.E., Reichard, G.A., Jr., Patel, M.S., and Boden, G. (1979). Energy metabolism in feasting and fasting. Adv. Exp. Med. Biol. *111*, 169–188.

Péterfy, M., Phan, J., Xu, P., and Reue, K. (2001). Lipodystrophy in the *fld* mouse results from mutation of a new gene encoding a nuclear protein, lipin. Nat. Genet. *27*, 121–124.

Phan, J., Péterfy, M., and Reue, K. (2004). Lipin expression preceding peroxisome proliferator-activated receptor-gamma is critical for adipogenesis *in vivo* and *in vitro*. J. Biol. Chem. *279*, 29558–29564.

Reue, K., Xu, P., Wang, X.P., and Slavin, B.G. (2000). Adipose tissue deficiency, glucose intolerance, and increased atherosclerosis result from mutation in the mouse fatty liver dystrophy (*fld*) gene. J. Lipid Res. *41*, 1067–1076.

Ross, S.R., Graves, R.A., Greenstein, A., Platt, K.A., Shyu, H.L., Mellovitz, B., and Spiegelman, B.M. (1990). A fat-specific enhancer is the primary

determinant of gene expression for adipocyte P2 *in vivo*. Proc. Natl. Acad. Sci. USA *87*, 9590–9594.

Schwartz, M.W., Woods, S.C., Porte, D., Jr., Seeley, R.J., and Baskin, D.G. (2000). Central nervous system control of food intake. Nature *404*, 661–671.

Seeley, R.J., and Woods, S.C. (2003). Monitoring of stored and available fuel by the CNS: implications for obesity. Nat. Rev. Neurosci. *4*, 901–909.

Seeley, R.J., Drazen, D.L., and Clegg, D.J. (2004). The critical role of the melanocortin system in the control of energy balance. Annu. Rev. Nutr. *24*, 133–149.

Son, C., Hosoda, K., Ishihara, K., Bevilacqua, L., Masuzaki, H., Fushiki, T., Harper, M.E., and Nakao, K. (2004). Reduction of diet-induced obesity in transgenic mice overexpressing uncoupling protein 3 in skeletal muscle. Diabetologia *47*, 47–54.

Tange, Y., Hirata, A., and Niwa, O. (2002). An evolutionarily conserved fission yeast protein, Ned1, implicated in normal nuclear morphology and chromosome stability, interacts with Dis3, Pim1/RCC1 and an essential nucleoporin. J. Cell Sci. *115*, 4375–4385.

Vidal-Puig, A.J., Grujic, D., Zhang, C.Y., Hagen, T., Boss, O., Ido, Y., Szczepanik, A., Wade, J., Mootha, V., Cortright, R., et al. (2000). Energy metabolism in uncoupling protein 3 gene knockout mice. J. Biol. Chem. *275*, 16258–16266.